Choose Your Color

From the Photonic Band Edge

Nonlinear Frequency Conversion

Michael Scalora, Mark J. Bloemer, Charles M. Bowden, Giuseppe D'Aguanno, Marco Centini, Concita Sibilia, Mario Bertolotti, Yannick Dumeige, Isabel Sagnes, Petar Vidakovic, and Ariel Levenson

Ordinary Bragg reflectors, also known as one-dimensional photonic band gap structures (PBGs), display extraordinary linear and nonlinear optical properties that present a remarkable opportunity: the simultaneous availability of exact phase matching conditions and field confinement that act together to yield significantly enhanced second and third harmonic generation, frequency down-conversion, and multi-wave mixing processes. This opens the door to a new class of micrometer-sized devices that represent a new generation of efficient parametric sources for up- and down-conversion processes.

Nonlinear optics is generally believed to have had its origins in the 1961 experiment by Franken and co-workers,[1] who detected 347-nm light at twice the frequency of a ruby laser beam after the beam had propagated through a quartz crystal. The researchers' enthusiasm was tempered by the rather low second harmonic conversion—~10^{-8} %—due to the difference between the phase velocities of the fundamental and second harmonic waves. The reaction of *Physical Review Letters* editors contributed to further mitigate their discovery. According to the account given by M.M. Fejer in Ref. [2], the editors thought the spot found on Franken's spectrographic plate was a flaw; their decision to remove it from the manuscript served in essence to eliminate the published evidence of the first experimental detection of second harmonic generation.

The power of the fundamental field (FF) Pω converted into the second harmonic (SH) $P_{2\omega}$ in a bulk material can be written as (see for example Ref. 3)

$$P_{2\omega} \alpha \frac{(\chi^{(2)})^2 P_\omega^2 L^2}{A} \frac{\sin^2(\Delta qL/2)}{(\Delta qL/2)^2} .$$

The following are the important parameters: L is the length of the medium; n_ω and $n_{2\omega}$ are the respective refractive indices at ω and 2ω; A is the cross-sectional area of the fundamental beam; and

$$\Delta q = \frac{2\omega}{c} (n_{2\omega} - n_\omega)$$

is the phase-mismatch that takes into account the difference between the phase velocities of the FF and SH waves. If $\Delta q \neq 0$, the 2ω field radiated by the oscillating dipoles induced by the FF can add together constructively only over the so-called "coherence length"

$$L_c = \frac{2\pi}{\Delta q} .$$

The coherence length is thus a measure of the maximum crystal length useful for producing second harmonic power. Under ordinary circumstances, as in Franken's experiment, the coherence length may be on the order of $L_c \sim 10\mu m$, although it can be even smaller, depending on the wavelength, as for III-V semiconductors, for example. This is true because in normally dispersive materials the refractive index increases with frequency and the condition of perfect phase matching, $\Delta q = 0$ and $n_\omega = n_{2\omega}$, in reality is never fulfilled.

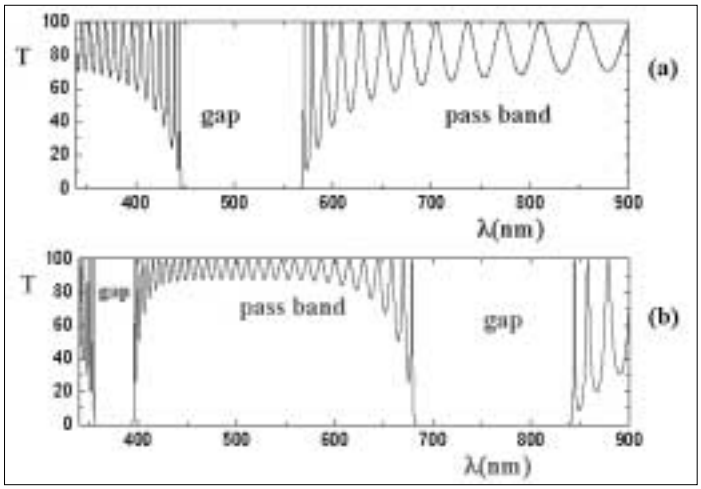

Figure 1. Transmission vs. wavelength for a 30-period AlN/SiO_2 (a) quarter-wave stack, and (b) half-wave/quarter-wave stack. Changing layer thickness amounts to modifying the effective dispersion of the stack, thus allowing phase matching between a FF and a SH beam to occur.

In Ref. 2, in which we also find a good historical review of nonlinear optical frequency conversion, the author discusses different stratagems employed over the years to overcome the inadequacies of conventional substances, material dispersion chief among them. Here we mention a few. For example, in 1962, Giordamaine[4] and Maker *et al.*[5] simultaneously proposed an ingenious method that led to the increase, to a few percent, of SH conversion efficiency. The technique used the difference between the refractive indices of waves with different polarizations in an optically anisotropic material such that the ideal condition $n_\omega = n_{2\omega}$ was better approximated. The possibility of matching the refractive indices of the second harmonic and fundamental waves by means of an anisotropy, which corresponds to increasing the coherence length, was experimentally demonstrated in the mid 1960s in potassium dihydrogen phosphate (KDP).[6,7] This method is still the most widely used for second harmonic generation in practical applications.

In 1962, Armstrong *et al.*[8] devised another method, now referred to as quasi phase matching (QPM). In QPM, a material of uniform, linear refractive index is characterized by a sign reversal of the nonlinear second order coefficient, $\chi^{(2)}$, every coherence length. Here, the generated second harmonic energy tends not to be reconverted back to the pump frequency as in ordinary, unmatched bulk materials, and conversion efficiencies are significantly improved over unmatched bulk materials. Because of the technological difficulties associated with the realization of the periodic inversion of $\chi^{(2)}$, experimental evidence of QPM improvements were not reported until the end of the 1970s. In 1970, Bloembergen and Sievers[9] proposed a different kind of phase matching, in which the linear properties of the structure itself could be used and controlled to compensate material dispersion for counter-propagating waves. This idea was shown to work in one-dimensional systems by Van der Ziel and Ilegems,[10] and by Trull *et al.*,[11] and in multidimensional systems by Martorell *et al.*[12]

QPM was first proposed in the 1960s, but multicolor generation (red, green, blue) using the scheme was first reported by Yamamoto *et al.* in 1991[13] in a proton-exchanged, MgO-doped, $LiNbO_3$ waveguide. The process exploited the Cerenkov configuration,[14] which provides QPM conditions over a wide range of wavelengths. Experiments demonstrated that QPM could be used to yield good conversion efficiencies for simultaneous multi-wavelength generation, relaunching the quest for realization of compact, multicolor laser sources for laser scanners, printers, and color display devices,[15-17] as well as other similar products. Although QPM made new types of materials available, to this day challenges remain because pumping intensities are far too high for practical applications.[2] For example, to even begin to deplete the pump, a 1cm long QPM sample with $\chi^{(2)}$ of order 10pm/V requires intensities of the order of 1GW/cm^2.

The purpose of this article is to draw attention to an alternative method of nonlinear frequency conversion that uses the simultaneous availability of field localization (a state with high energy density, or, put another way, high density of modes) and phase matching conditions near the one-dimensional photonic band edge.[18,19] These circumstances result in the effective enhancement of the nonlinear coefficient, and hence all related nonlinear frequency

1047-6938/01/04/0038/5-$0015.00

conversion processes, by several orders of magnitude with respect to either quasi phase matched or exactly phase matched bulk materials of similar length. Since a typical multilayer structure is only a few micrometers long, device length might stand to be significantly reduced, and material processing simplified.

When one thinks of a multilayer stack, a finite λ/4 dielectric Bragg reflector generally comes to mind. The layers alternate between a high and a low index of refraction, and most structures that we consider have a relatively small number of periods, typically 20 to 60. Because the structure is finite, the spectrum of transmitted light undergoes rapid oscillations that identify transmission resonances. Interference effects also cause portions of the spectrum to be completely reflected, giving rise to the so-called stop bands or band gaps. The bandwidth of the transmission resonance closest to the gap is roughly proportional to the index step between adjacent layers, and inversely proportional to the square of the number of periods.[20] The location of pass bands, resonances, and band gaps depends to a large extent on layer thickness. As an example, in Fig. 1 we show the transmission function of a 30-period, alternating AlN/SiO_2 quarter-wave stack for 550 nm (a), and that of a 30-period, AlN/SiO_2 half-wave/quarter-wave stack (b) vs. wavelength. In the latter case, the thicknesses of all high-index semiconductor layers have been changed to λ/2 for the same reference wavelength.

The two curves in Fig. 1 look similar in that they both have pass bands, transmission resonances, and gaps, and make rather dull mirrors. However, there are some important differences stemming from the different geometry. For example, the gap of one structure overlaps the pass band of the other: changing layer thickness amounts to shifting the relative position of pass bands and stop bands, a well-known effect. However, it is possible to view propagation of light through the finite stack as propagation in an effective medium.[19] When viewed within the context of an effective index of refraction that takes into account geometrical dispersion, the distinctive physical properties of each structure—

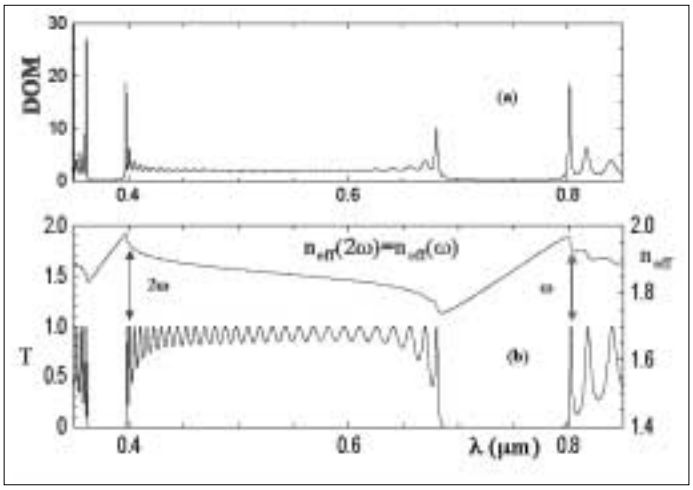

Figure 2. (a) Density of modes (DOM) for a 30-period AlN/SiO_2 optimized for phase matched SHG. The DOM is maximum at each transmission maximum. (b) The transmittance of the same structure is shown in blue; the effective index of refraction of the stack is shown in red. The optimized structure exhibits the same effective index of refraction at the first resonance near the low frequency (long wavelength) first order band edge, and at the second resonance of the long wavelength second order band edge, as indicated by the red and blue arrows.

properties that can be changed by changing layer thickness, i.e., geometrical dispersion—become apparent. The more important consequence is that geometrical dispersion can easily be manipulated and balanced against material dispersion to obtain exact phase matching between a pump and a generated second harmonic signal to a degree unforeseen in Ref. 9, a case in which it was accomplished for counter-propagating waves. In fact, since we are considering finite structures and our operating frequencies fall at resonances near the band edge, we can access states that possess global phase matching conditions, i.e., such that second harmonic generation is optimized for forward and backward waves. In addition, we can take advantage of the localization properties of the field, the intensity of which is enhanced by a factor proportional to the density of photon modes. For the typical structure that we consider, this enhancement factor ranges from one to two orders of magnitude compared with bulk materials.[18,19] Figure 2 shows the density of modes (a) and the transmittance (b) for an optimized 30-period AlN/SiO_2 half-wave/quarter-wave stack similar to that of Fig. 1. The density of modes plotted in Fig. 2a is normalized to the value of the density of modes in free space. Thus, near the band edges the structure provides a density of modes approximately 20-30 times larger than the density of modes of free space, and about 15 times larger than bulk AlN. For a periodic structure, the density of modes is proportional to the number of periods squared,[20] and thus its value is related to resonance bandwidth. We note that the transmittance maxima correspond to maxima in the density of modes, i.e., the structure provides the highest values of transmittance at frequencies at which the density of modes is highest. Since the pump intensity inside the structure is proportional to the density of modes,[18] it follows that the power converted to second harmonic frequency is enhanced by a factor proportional to the density of modes squared. Referring to the power formula above, this effect can also be viewed as an enhancement of the effective length of the structure and, as a result, we can reduce device length in proportion to the increase in the density of modes. For example, a 15-μm long structure, about 60 periods of AlN/SiO_2, has a density of modes approximately 60 times larger than the density of modes of bulk material (by doubling the number of periods the density of modes quadruples). This sample could therefore provide the same conversion efficiency as one millimeter of exactly phase matched bulk material. For longer interaction lengths, the simultaneous combination of exact phase matching conditions and local field enhancement in periodic structures can provide a remarkable increase in power conversion efficiency compared with bulk nonlinear crystals.

The first theoretical evidence of this effect in the case of second harmonic generation was reported in Ref. 18. The numerical simulations showed that a direct comparison between the conversion efficiency from a 20-period, 10-micrometer long GaAs/AlAs stack was some 500 times greater compared to the conversion efficiencies from an exactly phase matched GaAs bulk material also a few micrometers in length. Note however that this is only hypothetical because bulk GaAs cannot be phase matched due to the lack of birefringence. Nevertheless, we found that one could achieve the right balance between material and geometrical dispersion if the stack were pumped at 3 μm to generate

1.5-μm light. At shorter wavelengths, these materials are inadequate because their dispersion becomes too steep, and they quickly become absorptive. In Ref. 19 the results of the simulations were framed in terms of the effective index of refraction that we mentioned previously; this helps us better understand the predictions of large enhancement of conversion efficiencies. Later we will describe experimental results relating to this system.

It is easier to understand how exact phase matching can occur if we consider a periodic structure. In this case one can define the phase of the transmitted field for a periodic finite structure in terms of the Bloch phase β of the corresponding infinite, periodic structure.[20] At each transmission resonance, where T=100%, the phase of the transmitted field is precisely the Bloch phase, defined as

$$\beta_j = \frac{\pi}{N} j,$$

where *j* is an integer that corresponds to the *jth* resonance and *N* is the number of periods. For our effective index description of the periodic—but finite—stack,[19] the phase of the transmitted field, i.e., $\phi(\omega)=k(\omega)L$, where $k(\omega)=n_{eff}(\omega)\omega/c$, provides an effective dispersion relation.[19] For example, the phase of a pump field tuned to the first transmission resonance at the low frequency side of the first order gap, where the density of modes is high,[18,19] is given by

$$\beta(\omega)= \frac{\pi}{N} (N\text{-}1).$$

For a N-period structure, there are (N-1) resonances in the pass band between ω=0 and the first order gap. Therefore, the (*N*-1)*th* resonance corresponds with the first resonance near the low frequency band edge, or the 29th resonance counting from ω=0. Then, using the effective index approach, the phase matching condition that must be satisfied for second harmonic generation is simply $\beta(2\omega)=2\beta(\omega)$, or

$$\beta(2\omega)= \frac{\pi}{N} (2N\text{-}2).$$

This value restricts the phase matching condition for this periodic structure to the *(2N-2)th* resonance, *or the second resonance near the low frequency band edge of the second order gap.*[18,19] (See Fig. 2 for the identification of the transmission resonances that can provide the best conditions for second harmonic generation).

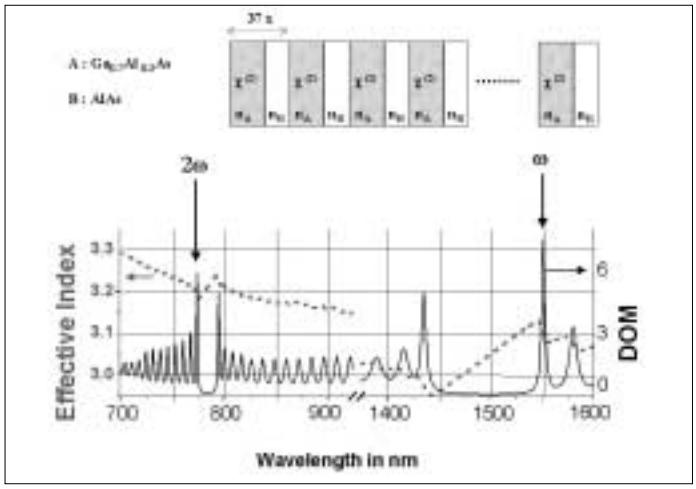

Figure 3. Density of modes (right axis) and effective refractive index (dotted in red, left axis) for the 37-period, $Ga_{0.7}Al_{0.3}As$/AlAs experimental sample. The dispersion is so steep that the SH frequency falls on the first resonance past the second order gap, as indicated by the arrow. In the figure we also provide a schematic representation of the stack. The stack parameters are: $n_A(\omega)= 3.231$; $n_A(2\omega)= 3.462$; $\chi^{(2)}$ (10°) = 10pm/V ; L_A = 136.8 nm ; and $n_B(\omega) = 2.902$; $n_B(2\omega)= 3.0149$; $\chi^{(2)}$ (10°) = 0 ; L_B = 108.5 nm.

Thus, the simple effective index model,[19] later extended to include nonlinear interactions,[21] predicted exact phase matching conditions for second harmonic generation—just as the simulations of the equations of motion had first suggested.[18] In the process, the effective index model also explained why maximum second harmonic conversion efficiency does not occur at an absolute maximum in the density of modes.[18] The message is that to maximize second harmonic generation, it is important to also consider the global phase matching conditions for the scattering event, which may or may not be optimal where the density of modes is at an absolute maximum. In Fig. 2 (b) we also show the behavior of the real part of the effective index of refraction for the 30-period AlN/SiO_2 structure optimized for second harmonic generation. The structure is designed by balancing geometrical and material dispersion to fulfill the phase matching condition between the *(N-1)th* and the *(2N-2)th* resonance. The determining factor that makes this work is the anomalous behavior of the index of refraction that generally occurs inside each gap, where the index tends to decrease. This reduction in the index compensates for the increasing index of bulk materials under conditions of normal dispersion, and phase matching can occur.

Strong experimental evidence for the kind of phase matching conditions and field localization described here is unfortunately still lacking from the published literature. This is not to say that experimental evidence is lacking. In fact, an experiment was recently performed at LPN Laboratory in France by Y. Dumeige and co-workers,[22] who used a GaAs/AlAs multilayer stack similar to that proposed in Ref. 18. The stack, schematically represented in Fig. 3, was designed for optimized second harmonic generation at 775nm. The nonlinear layer is $Ga_{0.7}Al_{0.3}As$ and the linear one is AlAs. At this wavelength, which is near the electronic band gap edge, material dispersion is quite steep for both materials: geometrical dispersion cannot fully compensate for material dispersion. Therefore, a compromise was reached such that a slight mismatch still existed between the effective refractive indices of the pump and generated field. The pump frequency was properly located at the first transmission resonance of the lowest energy photonic band gap to achieve the optimum mode density; however, the second harmonic frequency was tuned to the first transmission resonance on the opposite side of the second gap, as indicated in Fig.3. As a result, using the effective index model,[21] and a polarized FF, we predicted a conversion efficiency about 10 times (TM polarization) and 60 times (TE polarization) higher compared to the conversion efficiency from one coherence length of bulk $Ga_{0.7}Al_{0.3}As$, approximately 1.6 μm.[22] Although the experiment was performed in the undepleted pump regime and relatively far from optimum phase matching conditions, this result is still quite impressive; it suggests that at a minimum, a considerable reduction in typical device length can be contemplated.

In Fig. 4 we show the setup used in the experiment described above. An erbium-doped amplified pulsed fiber optic laser is used for the FF beam. Pulse duration and repetition rate are 8 ps and 20 MHz, re-

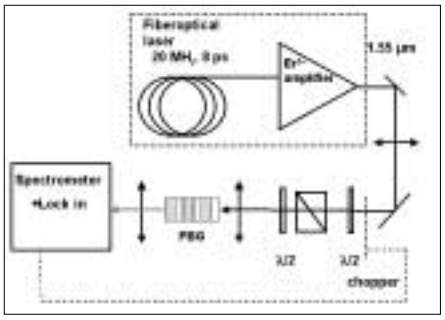

Figure 4. The setup used for the experiment. The bandwidth of the 8 ps pulses we used was much narrower compared to transmission resonance bandwidth. Longer pulses are better suited for this because they couple better with the structure, leading to higher local field intensities, as demonstrated in Ref. 18, and larger conversion efficiencies.

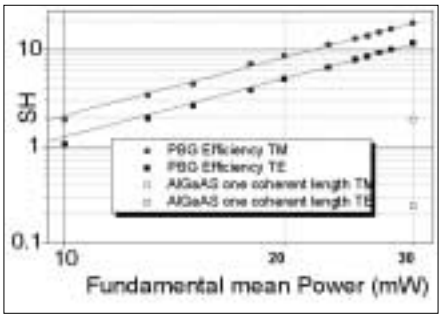

Figure 5. SH intensity as a function of the FF power. Filled circles (squares) correspond to a TM (TE) polarized FF. Also indicated are the values for one coherence length of $Ga_{0.7}Al_{0.3}As$.

spectively. A polarizer sandwiched between two half-wave plates is used to adjust both the FF intensity and polarization (TM or TE). In Fig. 5 we show the main results of the experiment for both TE and TM polarized pump pulses. The measured second harmonic signal from the multilayer stack is about 10 (for TM) and 50 (for TE) times more intense than the signal emanating from the one coherence length bulk $Ga_{0.7}Al_{0.3}As$, in close agreement with our predictions. Further experimental tests were performed in order to rule out other possible effects, such as surface or interface enhanced SHG. The experimental results thus strongly support the role played by photonic band edge effects in the enhancement of SHG.

Once the rules of the game are known, it becomes a simple matter to extend the model to fit other more complicated circumstances. For example, one can show that three wave mixing processes, such as parametric up- or down-conversion,[23] can occur under exact phase matching conditions. Under this category falls another remarkable effect, i.e., simultaneously phase matched second and third harmonic generation, briefly discussed in the 1960s[24] but never pursued because appropriate materials were thought not to exist. For the moment, however, although the experimental evidence goes a long way toward validating the concept, there is still a need to convincingly demonstrate a device that can be used to efficiently extract much coveted blue light from the photonic band edge. To do this, materials other than GaAs or AlAs must be used. For example, GaN and AlN[25] are good candidates since their dispersive properties can be controlled with the addition of geometrical dispersion, as Fig. 2 shows. Recent publications have shown reasonable nonlinear coefficients in AlN due to the columnar nature of the film growth, which provides the anisotropy required for the onset of second order nonlinearities.[26] Porous silicon[27] structures may also be fabricated and doped with a nonlinear material, then engineered to the desired specifications. Alternatively, one may resort to materials with relatively low nonlinear coefficients, and improve on the density of modes with modest increases in structure length.[20] This may require further refinement of growing and deposition methods. Finally, it is also possible to show that for second harmonic generation, modal dispersion may in principle be overcome in a periodically poled waveguide by superimposing an appropriate surface grating, i.e., by once again introducing and controlling geometrical dispersion.[28] Thus, we can have sample lengths on the order of centimeters along with the added benefits of increased density of modes and geometrically induced phase matching.

It therefore seems that photonic band gap structures may well constitute a leap forward in engineering new types of laser sources, in situations in which a series of effects combine to provide the desired phase matching conditions along with the enhancement of nonlinear frequency conversion. The process is based on judiciously combining and balancing geometrical and material dispersion. In practice, the method benefits from mature epitaxial growth and other well-known semiconductor processing technologies that make possible the production of structures with submicrometer period. Moreover, the effect remains efficient under a variety of tuning conditions characterized by small departures from exact phase matching.

References

1. P.A. Franken, A. E. Hill, C. W. Peters, G. Weinreich, Physical Review Letters **7**, 118 (1961).
2. M. M. Fejer, Physics Today **47**, 25 (1994).
3. Y. R. Shen, The Principles of Nonlinear Optics (John Wiley & Sons, New York, 1984).
4. J.A. Giordmaine, Physical Review Letters **8**, 19 (1962).
5. P.D. Maker, R. W. Terhune, M. Nisenoff, C. M. Savage, Physical Review Letters **8**, 21 (1962).
6. P.N. Butcher, T. P. McLean, Proc. Phys. Soc. **81**, 219 (1963).
7. H. Cheng, P. B. Miller, Physical Review **134**, A683 (1964).
8. J.A. Armstrong, N. Bloembergen, J. Ducuing, P.S. Pershan, Physical Review **127**, 1918 (1962).
9. N. Bloembergen and A. J. Sievers, Applied Physics Letters 17, 483 (1970).
10. J. P.Van der Ziel and M. Ilegems, Applied Physics Letters **28**, 437 (1976).
11. J. Trull, R. Vilaseca, J. Martorell, R. Corbalan, Optics Letters **20**, 1746 (1995).
12. J. Martorell, R. Vilaseca, R. Corbalan, Applied Physics Letters **70**, 701 (1997).
13. K. Yamamoto, H. Yamamoto, T. Taniuchi, Appl. Phys. Lett. **58**, 1227 (1991).
14. M.J. Li, M. De Micheli, Q.He, D.B. Ostrowsky, IEEE J. Quant. Elec. **26**, 1384 (1990).
15. X. Mu, X. Gu, M.V. Makarov, Y.J. Ding, J. Wang, J. Wei, Y.Liu, Opt. Lett. **25**, 117 (2000)
16. R. Ramponi, R. Osellame, M. Marangoni, V. Russo, E. Giorgetti, C. Xiafeng, A. Carta, F. Gelli, S. Sottini, in: Integrated Optics Devices IV, G.C. Righini and S. Honkanen eds, SPIE vol. P-3936, Washington D.C. (2000) 200-8.
17. Y.S. Kivshar, A.A. Sukhorukov, S.M. Saltiel, Physical Review E **60**, R5056 (1999).
18. M. Scalora *et al.*, Phys. Rev. A **56**, 3166 (1997).
19. M. Centini *et al.*, Physical Review E **60**, 4891 (1999).
20. J. M. Bendickson, J.P. Dowling, M. Scalora, Physical Review E **53**, 4107 (1996).
21. G. D'Aguanno *et al.*, Optics Letters **24**, 1663 (1999); G. D'Aguanno *et al.*, submitted to Physical Review.
22. Y. Dumeige *et al.*, submitted to Applied Physics Letters, 2000.
23. M. Centini *et al.*, Optics Communication **189**, 135 (2001); M. Centini *et al.*, submitted to Physical Review, 2001.
24. S.A. Akhmanov and R.V. Khokhlov, Gordon and Breach Science Publishers, 1972, NY. Translated from the original Russian edition: Problemy Nelineinoi Optiki, Academy of Sciences of the USSR, (1964).
25. H. M. Ng, T. D. Moustakas, and S. N. G. Chu, Applied Physics Letters **76**, 2818 (2000); D. Korakakis, K. F. Ludwig Jr., and T. D. Moustakas, Applied Physics Letters **72**, 1004 (1998).
26. G.T. Kiehne, G.K.L. Wong, J.B. Ketterson, Journal of Applied Physics **84**, 5922 (1998).
27. L.A.Golovan', A. M. Zheltikov, P. K. Kashkarov, N. I. Koroteev, M. G. Lisachenko, A. N. Naumov, D.A. Sidorov-Biryukov, V.Yu. Timoshenko, and A. B. Fedotov, JETP Letters **69**, 300 (1999).
28. J.W. Haus *et al.*, Physical Review A **57**, 2120 (1998); D. Pezzetta *et al.*, submitted to JOSA B.

Michael Scalora,[1,2] Mark J. Bloemer,[1] Charles M. Bowden,[1] Giuseppe D'Aguanno,[1,3] Marco Centini,[1,3] Concita Sibilia,[3] Mario Bertolotti,[3] Yannick Dumeige,[4] Isabel Sagnes,[4] Petar Vidakovic,[4] and Ariel Levenson[4] 1. U.S. Army Aviation & Missile Command, Weapons Sciences Directorate, AMSAM-RD-WS-ST Redstone Arsenal, AL, mscalora@ws.redstone.army.mil; 2. Time Domain Corporation, Huntsville AL; 3. Dipartimento di Energetica, La Sapienza, University of Rome, Rome Italy; 4. Laboratoire de Photonique et de Nanostructures, Bagneux France.